Journal of Applied Sciences 13 (1): 70-78, 2013
ISSN 1812-5654 / DOI: 10.3923/jas.2013.70.78

Variability of River Plume Signature Determined Using Satellite Images

A. Jabbar, T. Lihan, M.A. Mustapha, Z.A. Rahman and S.A. Rahim
School of Environmental and Natural Resource Sciences, Faculty of Science and Technology,
Universiti Kebangsaan Malaysia, Bangi, Selangor

Abstract: Estuarine outflow associated with suspended matter concentrations and pollutants have a major impact on marine ecosystems. Understanding the dynamics and dispersal pattern of suspended matter from river water are important for management of coastal water quality and biological productivity. This study aimed to determine the variability of Pahang River plume signature at the coastal area. One km spatial-resolution normalized water-leaving radiance, (nL_w 551) obtained from the Moderate Resolution Imaging Spectroradiometer (MODIS) on Aqua satellite were analyzed from the period of 2005-2010. The plume spectral signature estimated of the backscattering coefficient nL_w 551 (proxy for suspended matter) was strongly correlated with the amount of monthly average rainfall over the study period. The plume signature distributions during 2005-2010 based on nL_w 551 was highly variable. During northeast monsoon, the plume tends to propagate to the south and shows the strongest plume signature of nL_w 551 value (>2.0 mW cm^{-2} μm^{-1} sr^{-1}) meanwhile during southwest monsoon the plume dispersion to the north and exhibit weakest plume signature value (<1.5 mW cm^{-2} μm^{-1} sr^{-1}). The variability of plume signature was determined by the backscattering characteristics of surface waters in the region of the river mouth as a result of rainfall, wind stress and surface current event.

Key words: Coastal waters, interannual variability, nL_w 551, river plume, plume signature

INTRODUCTION

The estuarine outflow plume is a coastal process that provide a contrivance by which organic and inorganic materials connected to the river basin water will be transported into the continental shelf. The river plume which carries a mixture of fine silts, clays and dissolved organic matter into the coastal zone will directly affect the local shelfs physical, biogeochemical and ecological functioning (Thomas and Weatherbee, 2006). Additionally, river plume influences nutrient concentration and nutrient ratios in the water column and impact the benthic processes, productivity and pelagic life cycles (Miller and McKee, 2004; Dzwonkowski and Yan, 2005; Thomas and Weatherbee, 2006; Lihan *et al*., 2011). The plume that settled in the vicinity of the river mouth is a major source of pollutants and pathogens that flows out to the sea. In fact these plumes can also have a negative impact on humans, ecosystem health and productivity (Lihan *et al*., 2008).

A typical plume event begins with a force and momentum injection of river discharge to propagate the river plume onto the near-shore shelf. These outflows can develop into relatively large sizes and travel in along-shore for several kilometers (Dzwonkowski and Yan, 2005). The knowledge of river plume dynamics to date is based on data gathered from shipped-based surveys (Nezlin and DiGiacomo, 2005). The distribution patterns of river plume events can be related to a number of factors including magnitude and direction of wind stress, ocean current and discharge strength. This various nature factors can raise complications in monitoring plume events by traditional approaches such as mooring arrays and shipboard surveys (Johnson *et al*., 2001). Moreover, it is difficult to study the plume dynamic patterns from field measurements due to limited coverage area, sampling logistics cost and unpredictable weather (Nezlin and DiGiacomo, 2005). The use of remotely sensed data has provided unprecedented views of a wide range of river plume evolution processes on various spatial and temporal scales (Dzwonkowski and Yan, 2005). This enables more effective analysis of the distribution patterns of river plume that can be measured from space (Nezlin *et al*., 2005).

Satellite imagery compromises an alternative approach for plume properties assessment. Several

Corresponding Author: Tukimat Lihan, School of Environmental and Natural Resource Sciences, Faculty of Science and Technology, Universiti Kebangsaan Malaysia, 43600 Bangi, Selangor, Malaysia Tel: +603-89214051 Fax: +603-89253357

studies used satellite imagery to track plume dynamic patterns structure over time. Ocean color is well correlated with important plume characteristics such as salinity and suspended matter (Nezlin *et al*., 2007). In this study ocean color data was used to determine the variability of the Pahang River plume signature. Typical outflow plumes are best characterized by their signature of decreased salinity of estuarine water composition (Dzwonkowski and Yan, 2005; Nezlin and DiGiacomo, 2005). Unfortunately salinity presently cannot be measured from space by satellite platforms. However, previous studies have shown that river plume which carries dissolved organic materials and suspended matter allow plume events to be recognized by remotely sensed optical images (Johnson *et al*., 2003). Therefore it is important to understand the spectral distribution of Pahang River plume signature. This can be accomplished by using MODIS images to clarify the spectral reflectance dynamics of the Pahang River plume. The knowledge of the factors regulating plume dynamics is fundamental because the presence of river plume will restrain primary productivity due to reduction in the photic depth. This will eventually have important implications for coastal fisheries activities (Lihan *et al*., 2011). This study aims to determine the variability of the Pahang River plume signature distributions using ocean color satellite images.

MATERIALS AND METHODS

Study area: The Pahang River system is vital in the irrigation of agriculture in the vicinity of Pahang Basin. Pahang River consists of 16 major rivers with a total length of 440 km. It is the longest river in Peninsular Malaysia and flows into South China Sea at Pekan (Fig. 1). The South China Sea experiences two distinct monsoons throughout the year which are northeast monsoon (November to May) and southwest monsoon (May to September) while two inter-monsoon in April and October. This monsoonal climate strongly affects circulation and wind which in turn influences the water content of Pahang River plumes.

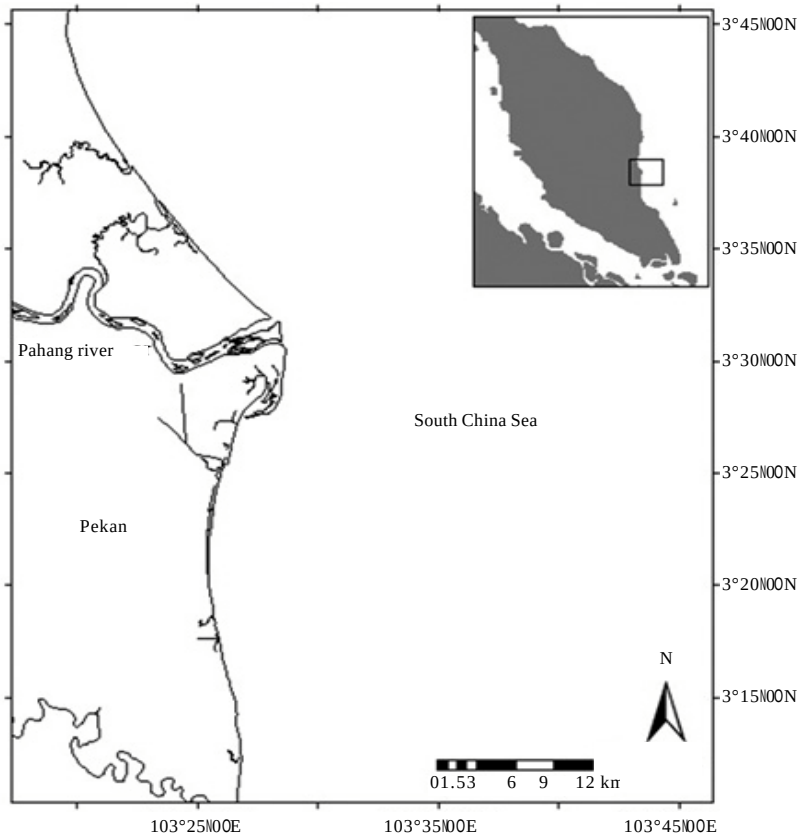

Fig. 1: Study area at the coastal of Pahang river mouth

In this study, a river plume is defined as a water mass with a spectral reflectance different from that of the ambient water masses (Nezlin and DiGiacomo, 2005). This was measured using the values of normalized water-leaving radiation at a wavelength of 551 nm (nL_w 551) derived from Moderate Resolution Imaging Spectroradiometer (MODIS) images. The nL_w 551 have been adopted to determine the plume signature patterns due to its ability to describe the suspended particulate matter effectively (Li *et al*., 2003). An identical spatial reference is required to precisely compare the spatial features in the data used of this study. The coastline of the study area was used as a base map to which all other data were projected with a Mercator system identical to that the base map. The combination of remote sensing imagery and ancillary data such surface wind, surface current and rainfall were used to evaluate the influence of these multi nature factors on the regulating river plume signature variability.

Satellite data: The satellite data used in this study were derived from Aqua-MODIS sensor, available in Level 1A MODIS swaths intersecting the region of 0-10°N, 100-120°E for the period of January 2005 to December 2010. These data were downloaded from NASA Goddard Space Flight Center Distributed Active Archive Center and processed to level 2 geophysical products using NASA coefficients and community-standard algorithms as implemented by SeaWiFS Data Analysis System (SeaDAS version 6.1) software. The radiances measured by the satellite sensors (MODIS) were converted into normalized water-leaving radiances (nL_w). These data were further processed using a combined NIR-SWIR atmospheric correction approach (Shi and Wang, 2007; Wang and Shi, 2007). MODIS imagery basically is based on two NIR bands used for recognizing the aerosol type and correcting aerosol contributions at the visible wavelengths (Gordon and Wang, 1994; Gordon, 1997). The atmospheric correction was based on an aerosol model, utilizing the shortest infrared wavelength at 1240 nm and the longest infrared wavelength at 2130 nm, because ocean surface reflectance in SWIR is close to zero regardless of suspended matter and CDOM concentrations (Wang and Shi, 2005; Wang, 2007; Nezlin *et al*., 2008; Lahet and Stramski, 2010). However, the MODIS SWIR was deliberated for the land and atmosphere applications with significantly lower sensor band Signal-Noise Ratio (SNR) values. For better result of ocean color products, superior sensor SNR values for SWIR bands are requisite. Therefore, a combined of NIR-SWIR method (Shi and Wang, 2007; Wang and Shi, 2007) was used for the MODIS ocean color data processing. Combination of NIR and SWIR method of atmospheric correction will compute a turbidity index based on MODIS-measured radiances at the NIR and SWIR bands to discriminate between turbid coastal and non-turbid ocean waters (Shi and Wang, 2007). The normalized water-leaving radiances nL_w 551 L2 product were remapped to a cylindrical projection at 1000 m spatial resolution. A total of 1090 nL_w 551 daily data were further composited into monthly means, as well as monthly climatology for the six year periods using ERDAS IMAGINE version 2010 software.

Surface wind data: Gridded monthly surface wind data were downloaded from NOAA Earth System Research Laboratory website (http://www.esrl.noaa.gov). These files contain regular grids of zonal (onshore) and meridonal (alongshore) wind speeds at 10 m above the earth surface to characterize the wind forcing for the study period. The direction and magnitude of the wind surface were analyzed using the grid analysis and display system (GrADS) and this data were transformed to wind stress, τ (kg m^{-1} sec^{-2}) with the equation:

$$\tau = C_d \rho_{air} U^2$$

where, C_D is the dimensionless drag coefficient (0.0013), ρ_{air} is the air density (1.22 kg m^{-3}) and U is the wind speed at 10 m above surface (Nezlin and DiGiacomo, 2005; Lihan *et al*., 2008).

Surface current data: Gridded monthly ocean surface currents with 1 degree resolution were acquired from Ocean Surface Current Analysis (OSCAR) model (Bonjean and Lagerloef, 2002) at the National Ocean and Atmospheric Administration (NOAA) (http://www.oscar.noaa.gov). The zonal and meridonal components data from 2005 to 2010 were analyzed in GrADS.

Rainfall data: A time series of daily Kuala Pahang (near to the river mouth) rainfall data from 1 January 2005 to 31 December 2010 were obtained from Malaysian Meteorology Department. Rainfall data were used to evaluate the influence of river discharge on the river plume signature variability. Correlation between rainfall and the nL_w 551 values detected by satellite was examined using a model of the linear signal/response dependence between these two parameters.

RESULTS

The optical properties of Pahang River plume signature shows strong variability in time and space. The distribution patterns of plume signature is consistent with rainfall, surface wind and surface current being dominant influences to the variability. Interannual variability of spatial plume signature shows four distinct formations at the mouth of the Pahang River. The nL_w 551 was used, assumed to be an effective tracer to determine the distributions of suspended particulate matter in water body at coastal area.

Rainfall: Pahang river basin in general experiences high intensity of rainfall during wet season (northeast monsoon) in November-March each year. In contrast a low distribution of precipitation occurs during dry season (southwest monsoon) in May-September. Based on the monthly average rainfall climatology data, the highest average of rainfall was recorded in October to December (>10 mm) while the minimal influences of precipitation was in June and July (<5 mm) during the six years of study period (Fig. 2).

Throughout the study period, Pahang coastal area receives highest intensity of rainfall in December 2009 (29.20 mm) followed by November 2010 with 19.88 mm of average rainfall. The lowest intensity of rainfall was recorded in February 2010 (0.85 mm) and the second lowest was recorded in July 2009 (1.03 mm) (Fig. 3).

Plume signature: The nL_w 551 value climatology data showed a similar pattern with rainfall which distributed highest in November-March and lowest in June to September through 2005-2010 (Fig. 2). The climatological data of nL_w 551 value showed that the spectral signature of Pahang River had the highest reflectance in 551 nm wavelength during November with the radiance values exceeding more 1.54 mW cm^{-2} μm^{-1} sr^{-1} and increased to 3.2 mW cm^{-2} μm^{-1} sr^{-1} in December. In late northeast monsoon, the plume signature value decreased to less than 2.46 mW cm^{-2} μm^{-1} sr^{-1}. In the early of southwest monsoon (May), the spectral signature exhibited a lower reflectance (<1.5 mW cm^{-2} μm^{-1} sr^{-1}) at this short wavelength. Until the end of southwest monsoon (September) the spectral signature showed that lower reflectance was detected which was between 1.2-1.5 mW cm^{-2} μm^{-1} sr^{-1}.

Interannual variability of spatial plume signature patterns observed during the study period were distributed into four distinct formation at the mouth of the Pahang River and the coastal area which exhibits along the coast, directed to the south, propagated offshore and distributed to the north (Fig. 3). Based on the plume signature seasonal cycle in Fig. 3, red area reflects on the high value of suspended material and blue indicates the low value of suspended material detected by nL_w 551. The nL_w spectral signature of plume distribution during 2005 to 2010 was highly variable and dependent on the monthly rainfall. The highest radiance value of plume signature recorded during this study period was observed in November 2006 (4.2 mW cm^{-2} μm^{-1} sr^{-1}) and the second highest radiance value was recorded in December 2008 (3.7 mW cm^{-2} μm^{-1} sr^{-1}). The lowest reflectance of plume signature recorded was 0.9 and 1.1 mW cm^{-2} μm^{-1} sr^{-1} in August 2005 and August 2006, respectively (Fig. 4). Linear correlation analysis was

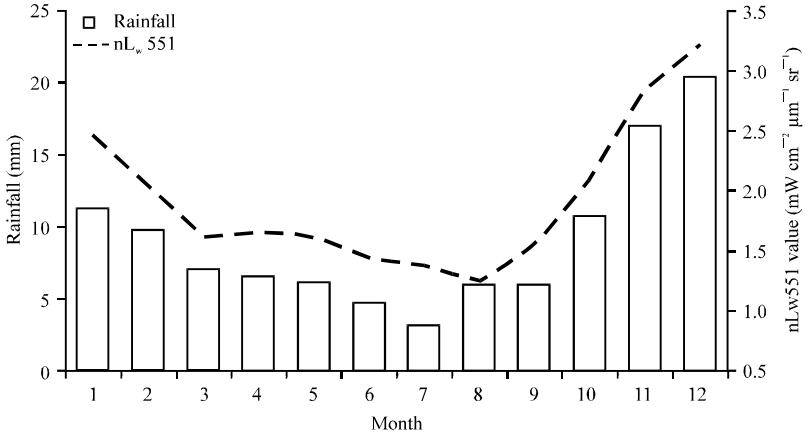

Fig. 2: Climatology of monthly average rainfall and monthly average nL_w 551 radiance value over 6-year study period (2005-2010)

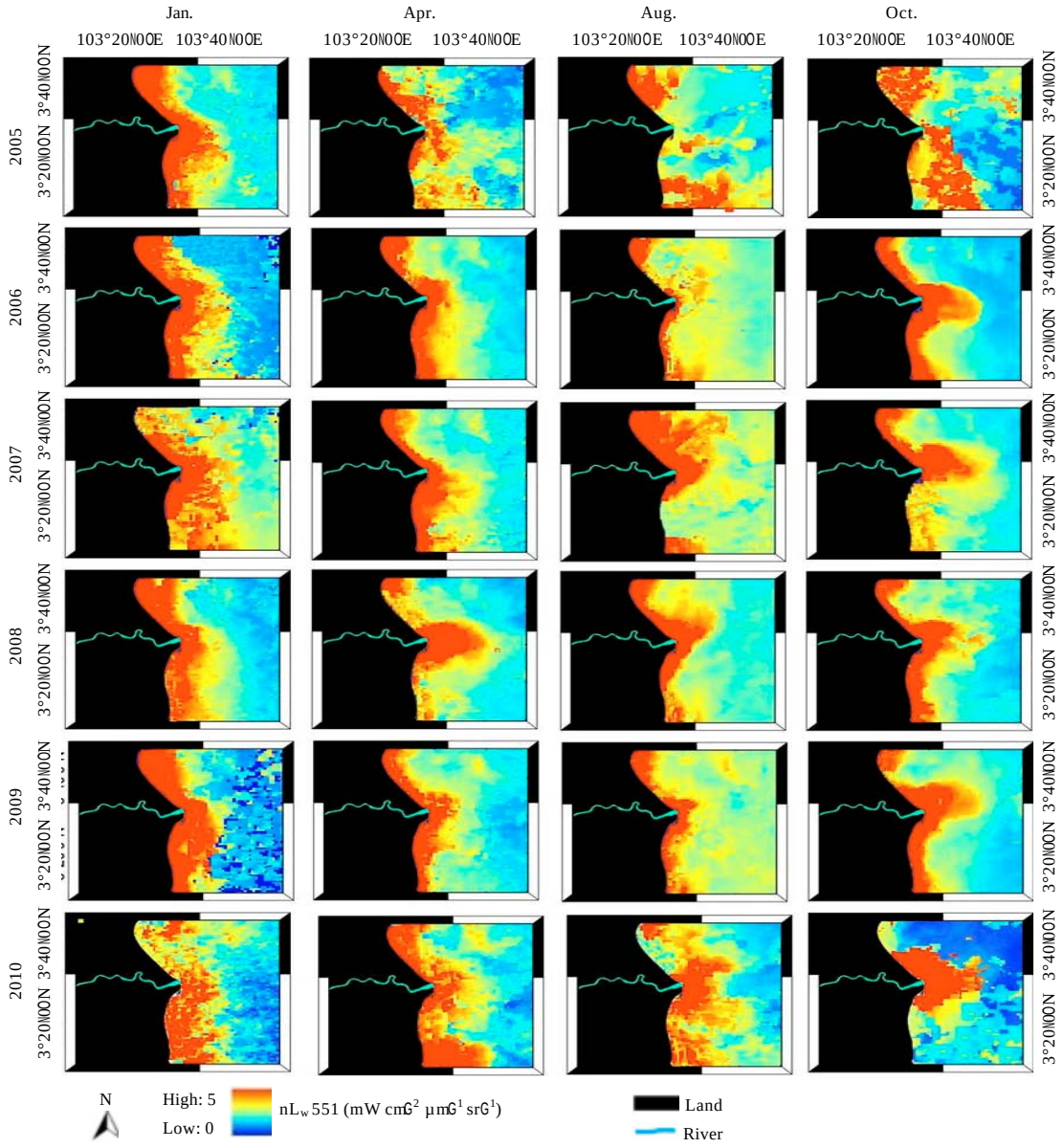

Fig. 3: Seasonal cycle of plume distribution patterns over 6-years in the normalized water-leaving radiance at 551 nm (nL_w 551), an effective tracer of suspended particulate matter in the coastal vicinity. The time series show the progression in plume movement and formation at coastal area during (Jan.) northeast monsoon, (Apr.) inter-monsoon, (Aug.) southwest monsoon and (Oct.) inter-monsoon

performed to investigate the influence of precipitation on the plume signature radiance nL_w 551 value. Linear correlation analysis indicated positive correlation ($r = 0.79$ $n = 72$) between nL_w 551 value and monthly average rainfall suggesting that normalized water-leaving radiance (nL_w 551) is a good proxy of freshwater plume along the Pahang River coastal area.

Wind stress and surface current: River plume signature variability associated positively with a wind stress and current other than rainfall. Analysis of the wind stress data shows high magnitude of wind stress forcing occurred in November to February every year during 2005-2010. The highest magnitude of wind stress was recorded in January 2007 (0.10 kg m^{-1} sec^{-2}) and the

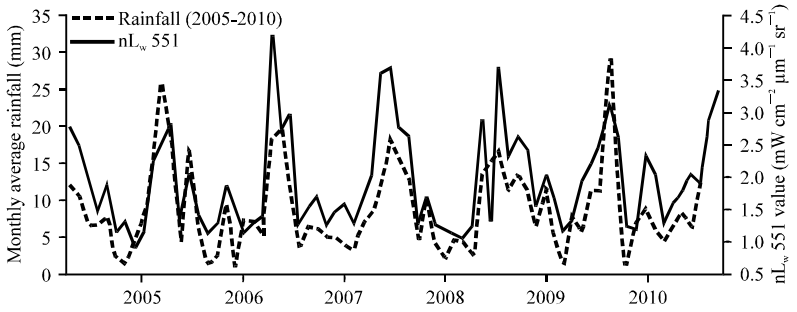

Fig. 4: Relationship between time series of monthly average rainfall for 2005-2010 with nL_w 551 radiance value throughout the study period

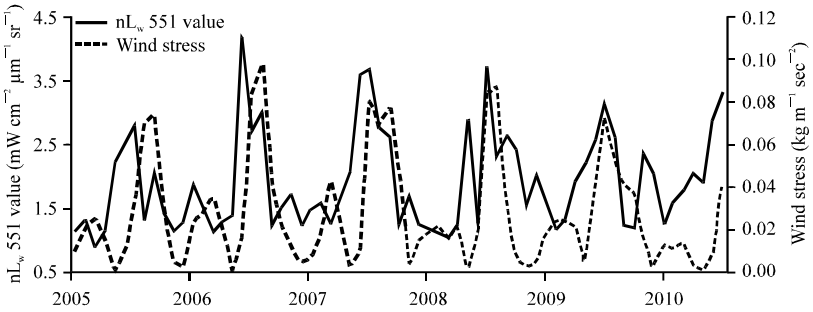

Fig. 5: Time series of monthly wind stress and nL_w 551 throughout the study period (2005-2010). Strong wind stress and nL_w 551 radiance value observed during northeast monsoon and weak wind stress and nL_w 551 radiance value occurring during southwest monsoon

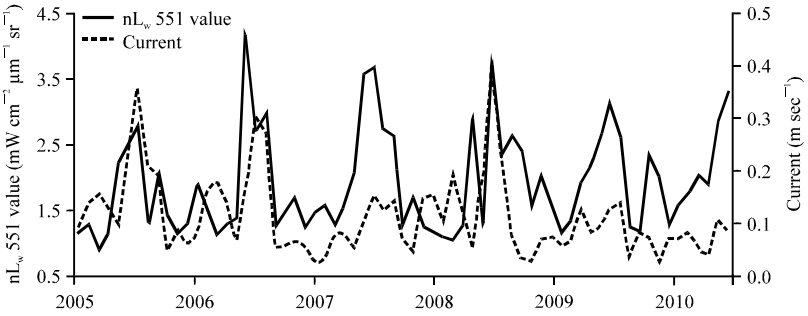

Fig. 6: Time series of monthly ocean surface current and nL_w 551 throughout the study period (2005-2010), Strong ocean surface current and nL_w 551 radiance value observed during northeast monsoon and weak ocean surface current and nL_w 551 radiance value occurring during southwest monsoon

second highest in January 2009 (0.09 kg m^{-1} sec^{-2}). The lowest magnitude of wind stress was observed in October 2006 (0.0002 kg m^{-1} sec^{-2}) followed by October 2010 (0.0006 kg m^{-1} sec^{-2}) (Fig. 5). Meanwhile, strong velocity of surface current occurred in November to January each year during the study period. The strongest velocity of surface current was observed in December 2005 (0.36 m sec^{-1}) and 2008 (0.38 m sec^{-1}). The weakest velocity of surface current was recorded in May 2010 and the second weakest recorded in June 2006 both with the value of 0.02 m sec^{-1} (Fig. 6).

DISCUSSION

The seasonal evolution and translocation of Pahang River plume distribution dynamics which are associated

to wind stress and surface currents are described using the monthly time series of nL_w 551. The plume signature distribution pattern in front of the river mouth during this study period is affected from the precipitation, wind stress and local surface current which is regulated by the monsoon for certain period (Fig. 4-6).

During Nov. and Dec. (northeast monsoon) the plume extends further to offshore and begins to distribute southward with highest plume signature values of nL_w 551 (1.50-3.00 mW cm^{-2} μm^{-1} sr^{-1}). A strong wind stress (0.01-0.09 kg m^{-1} sec^{-2}) pushes the offshore plume and directed it to the south. Strong local circulation force (0.3> m sec^{-1}) also aids the plume to disperse southward of river mouth. During this monsoon, east coast of Peninsular Malaysia experiencing a heavy rain which can extends to eight days. Continuous heavy rains for a period of time will cause flooding. In the northeast northeast monsoon the discharges of Pahang River is at its peak which in turn reflect the high spectral reflection in estuaries and coastal areas. The strong plume signature was most likely due to the backscatter from dissolved and suspended particles which include suspended sediment, phytoplankton and Colored Dissolved Organic Matter (CDOM) or yellow substance derived from land use activities at the river basin (Lahet *et al*., 2001; Bowers *et al*., 2004). After water masses of estuarine leaving river mouth to reach shelf region, the dissolved and suspended material become limited.

Pahang coastal area is still experiencing the northeast monsoon and the suspended matter from the plume is oriented strongly to the south and the nL_w values reflect the sum of both organic and inorganic material is <2.4 mW cm^{-2} μm^{-1} sr^{-1} during January to March. The effect of northeast monsoon is almost at the end and yet the plume can extend up to 30 km to the south part of coastal area. The northeast wind with strong magnitude is still dominant during January to March (0.07-0.09 kg m^{-1} sec^{-2}), pushing the river plume to south. In addition, the presence of a strong velocity (1.5-2.7 m sec^{-1}) of ocean current which circulates to the south facilitates the transportation of the plume even further to the southward. The strong value of nL_w 551 exhibited during this period might be associated with re-suspension of suspended matter at the bottom of estuary by the combination of strong wind mixing and current event which also reported by Hetland (2005) and Walker *et al*. (2005).

In April, the nL_w 551 radian values exhibit an average reflectance (1.6 mW cm^{-2} μm^{-1} sr^{-1}) along-shore and the dispersion of the plume can extend within the distance of 25 km of the coastal region shelf, starting from river mouth. During the inter-monsoon in April, the wind stress (east wind) and the current are relatively strong and not exceeding 0.01 kg m^{-1} sec^{-2} and 0.08 m sec^{-1}, respectively which in turn caused the plume to spread over a wide region.

Plume signature patterns in May-September indicated that the plume oriented offshore and propagated to north. During May-September (southwest monsoon), the plume rarely extends further than 21 km offshore, north of Pahang River mouth. During the southwest monsoon, the plume was directed to the north due to the southwest wind. At the beginning of the southwest monsoon (May) the magnitude of the wind stress is relatively weak (0.005-0.01 kg m^{-1} sec^{-2}), but become stronger at the end of the monsoon which can exceed 0.03 kg m^{-1} sec^{-2}, pushing the plume northward. The plume signature was observed during southwest monsoon were weakest with nL_w 551 value less than 1.5 mW cm^{-2} μm^{-1} sr^{-1} because the suspended material within the water column over the shelf that are not obviously associated with turbid plume due to low river discharge (low precipitation).

In October, during the transition of dry season to wet season the plume propagated offshore and extended to the sea. During this period, the plume signature values increased to 2.00 mW cm^{-2} μm^{-1} sr^{-1} indicating the transition from dry to wet season. The wind stress and surface current forcing during the inter-monsoon in October were the weakest which were 0.0006 kg m^{-1} sec^{-2} and 0.060 m sec^{-1}, respectively. According to Lahet *et al*. (2001) and Lihan *et al*. (2008), when the river plume water body lacks of dissolved and suspended material, it is characterized by low reflectance of visible wavelengths. During the six year of study periods, the Pahang River recorded the lowest average of rainfall in July and September (dry season). During this period the river discharge is very low due to the low intensity of precipitation. This condition will cause the influence of river discharge to carry out dissolved substances, suspended sediments, phytoplankton and Colored Dissolved Organic Matter (CDOM) or yellow substance of the river plumes from the river mouth weakened and could be the evidences to the low spectral reflectance displayed of plume signature at the time.

CONCLUSIONS

This study provides the best conceptual ocean color to understand the seasonal differences in the strength and position patterns of the Pahang River plumes signature which have a significant influence in surrounding ecosystem as sediment deposition will effect on water body stratification. The Pahang River plume shows high variability in signature pattern, distributed

into four distinct formation at the river mouth. During the southwest monsoon the plume signature value of nL_w 551 were weakest and extend to the north. Meanwhile in northeast monsoon the plume signature value of nL_w 551 were strongest and propagated to the south. The plume signature of nL_w 551 variability patterns was influenced by the rainfall, magnitude of surface current and wind stress that come along during both dominance seasons. Future works will focus on collection of incident in-situ data, determine the interannual variability of plum size, character, strength and primary productivity to further increasing the utility of satellite multispectral data in monitoring environmental issues of Pahang River plume.

ACKNOWLEDGMENTS

This study is part of a research project funded by the Ministry of Science, Technology and Innovation (MOSTI), Malaysia under the grant No. 04-01-02-SF0589. We thank the Distributed Active Archive Center at the NASA Goddard Space Flight Center for the production and distribution of the MODIS data and NOAA Earth System Research Laboratory and Ocean Surface Current Analysis for the wind and current data. We also thank the Malaysian Meteorology Department for the rainfall data. Special recognition to honor the National University of Malaysia (UKM) for providing financial support to carry out this research work and for the provision of the research facilities, technical and assistance.

REFERENCES

Bonjean, F. and G.S.E. Lagerloef, 2002. Diagnostic model and analysis of the surface currents in the tropical pacific ocean. J. Phys. Oceanogr., 32: 2938-2954.

Bowers, D.G., D. Evans, D.N. Thomas, K. Ellis and P.J.B. Williams, 2004. Interpreting the colour of an estuary. Estuar. Coast. Shelf. S., 59: 13-20.

Dzwonkowski, B. and X.H. Yan, 2005. Tracking of a Chesapeake Bay estuarine outflow plume with satellite-based ocean color data. Cont. Shelf. Res., 25: 1942-1958.

Gordon, H.R. and M. Wang, 1994. Retrieval of water-leaving radiance and aerosol optical thickness over the oceans with SeaWiFS: A preliminary algorithm. Applied Optics, 33: 443-452.

Gordon, H.R., 1997. Atmospheric correction of ocean color imagery in the earth observing system era. J. Geophys. Res. Atmos., 102: 17081-17106.

Hetland, R.D., 2005. Relating river plume structure to vertical mixing. J. Phys. Oceanogr., 35: 1667-1668.

Johnson, D.R., A. Weidermann, R. Arnone and C.O. Davis, 2001. Chesapeake Bay outflow plume and coastal upwelling events: Physical and optical properties. J. Geophys, Res., 106: 11613-11622.

Johnson, D.R., J. Miller and O. Schofield, 2003. Dynamics and optics of the Hudson River outflow plume. J. Geophys. Res., 108: 3323-3332.

Lahet, F. and D. Stramski, 2010. MODIS imagery of turbid plumes in San Diego coastal waters during rainstorm events. Remote Sens Environ., 114: 332-344.

Lahet, F., S. Ouillon and P. Forget, 2001. Colour classification of coastal waters of the Ebro river plume from spectral reflectances. Int. J. Remote. Sens., 22: 1639-1664.

Li, R.R., Y.J. Kaufman, B.C. Gao and C.O. Davis, 2003. Remote sensing of suspended sediments and shallow coastal waters. IEEE Trans. Geosci. Remote Sens., 41: 559-566.

Lihan, T., S.I. Saitoh, T. Iida, T. Hirawake and K. Iida, 2008. Satellite-measured temporal and spatial variability of the Tokachi River plume. Estuarine Coastal Shelf Sci., 78: 237-249.

Lihan, T., M.A. Mustapha, S.A. Rahim, S. Saitoh and K. Iida, 2011. Influence of river plume on variability of chlorophyll a concentration using satellite images. J. Applied Sci., 11: 484-493.

Miller, R.L. and B.A. McKee, 2004. Using MODIS Terra 250 m imagery to map concentration of total suspended matter in coastal waters. Remote Sensing Env., 93: 259-266.

Nezlin, N.P. and P.M. DiGiacomo, 2005. Satellite ocean color observations of stormwater runoff plumes along the San Pedro Shelf (Southern California) during 1997-2003. Continental Shelf Res., 25: 1692-1711.

Nezlin, N.P., P.M. DiGiacomo, D.W. Diehl, B.H. Jones and S.C. Johnson *et al*., 2008. Stormwater plume detection by MODIS imagery in the Southern California coastal ocean. Estuar. Coast. Shelf Sci., 80: 141-152.

Nezlin, N.P., P.M. DiGiacomo, E.D. Stein and D. Ackerman, 2005. Stormwater runoff plumes observed by SeaWiFS radiometer in the Southern California Bight. Remote Sens. Environ., 98: 494-510.

Nezlin, N.P., S.B. Weisberg and D.W. Diehl, 2007. Relative availability of satellite imagery and ship-based sampling for assessment of stormwater runoff plumes in coastal southern California. Estuar. Coast. Shelf. Sci., 71: 250-258.

Shi, W. and M. Wang, 2007. Detection of turbid waters and absorbing aerosols for the MODIS ocean color data processing. Remote Sens. Environ., 110: 149-161.

Thomas, A.C. and R.A. Weatherbee, 2006. Satellite-measured temporal variability of the Columbia River plume. Remote Sensing Environ., 100: 167-178.

Walker, N.D., W.J. Wiseman Jr., L.J. Rouse Jr. and A. Babin, 2005. Effects of river discharge, wind stress and slope eddies on circulation and the satellite-observed structure of the Mississippi River plume. J. Coastal. Res., 21: 1228-1234.

Wang, M. and W. Shi, 2005. Estimation of ocean contribution at the MODIS near-infrared wavelengths along the east coast of the U.S: Two case studies. Geophys. Res. Lett., 32: L13606-L13611.

Wang, M. and W. Shi, 2007. The NIR-SWIR combined atmospheric correction approach for MODIS ocean color data processing. Opt. Express, 15: 15722-15733.

Wang, M., 2007. Remote sensing of the ocean contributions from ultraviolet to near-infrared using the shortwave infrared bands: Simulations. Applied Optics, 46: 1535-1547.